May 16th, 4:20 PM

Characterization of Two-Phase Flows in Plunge Pools

Jose M. Carrillo
Universidad Politecnica de Cartagena, jose.carrillo@upct.es

Luis G. Castillo
Universidad Politecnica de Cartagena, luis.castillo@upct.es

Francisca Marco
Universidad Politecnica de Cartagena, francisca.marco@upct.es

Juan T. García
Universidad Politecnica de Cartagena, juan.gbermejo@upct.es

Recommended Citation

Carrillo, Jose (2018). Characterization of Two-Phase Flows in Plunge Pools. Daniel Bung, Blake Tullis, 7th IAHR International Symposium on Hydraulic Structures, Aachen, Germany, 15-18 May. doi: 10.15142/T3JM1W (978-0-692-13277-7).

7th International Symposium on Hydraulic Structures Aachen, Germany, 15-18 May 2018
ISBN: 978-0-692-13277-7 DOI: 10.15142/T3JM1W

Characterization of Two-Phase Flows in Plunge Pools

J.M. Carrillo[1], L.G. Castillo[1], F. Marco[1] & J.T. García[1]
[1]*Hidr@m Group, Universidad Politécnica de Cartagena, Cartagena, Spain*
E-mail: jose.carrillo@upct.es

Abstract: *The increasing magnitude of design floods has prompted re-evaluations of spillway capacity for large dams throughout the world. Current capacity of many spillways is inadequate. The overtopping creates new loading scenarios for the dam and raises questions about erosion and scour downstream from the dam. In this study, mean velocity was measured in different sections of the falling jet with optical fiber and with LS-PIV (Large Scale – Particle Image Velocimetry). Detailed studies of the submerged hydraulic jump downstream overflow nappe impinging jets are scarce. This work addresses such a situation, and compares numerical results against our own experiments. To advance the understanding of the phenomenon, instantaneous velocity was measured in the plunge pool with Acoustic Doppler Velocimeter (ADV) equipment, and mean velocities and air entrainment rate were obtained with optical fiber instrumentation. At the same time, transient numerical simulations were carried out with computational fluid dynamics (CFD) programs. Due to the variation of the air concentration in the plunge pool, optical fiber obtained valid velocities near to the impingement point, while ADV was used once the air concentration was small, allowing for the measurement of the velocity in the whole submerged hydraulic jump. In general, the CFD simulations provided results fairly close to the laboratory values measured, in spite of having used a simple two-phase flow model.*

Keywords: *air-water flow, energy dissipation, falling jets, numerical simulations, overtopping, plunge pool.*

1. Introduction

In recent years, the increase in the magnitude of design floods has promoted the revaluation of the spillways capacity and the operational scenarios for large dams around the World. Several studies have shown that the current capacity of many spillways is inadequate, and dams may overflow during extreme events. Increasing the capacity of spillways is costly and sometimes technically impracticable. In these cases, the dams' owners could consider the overflow as an additional strategy of operation during extreme events. This situation creates new loading scenarios, raising questions about the hydrodynamic actions and scour downstream of the dams (Wahl et al., 2008; FEMA, 2014).

The choice of the type of plunge pool is usually a technical-economic decision between a deep and uncoated stilling basin and a shallow stilling basin with lining. It is necessary to know the magnitude and frequency of the dynamic pressure in the bottom of the plunge pool. The required water cushion depth depends on the characteristics of the impingement jet so that most of the energy is dissipated, avoiding scour downstream of the dam (Annandale, 2006). The energy dissipation mechanisms in the free-flow jets can be divided into the following (Fig. 1a): (a) aeration and disintegration of the jet during its fall, (b) entrainment of air and diffusion of the jet in the water cushion, (c) impact on the basin bottom, and (d) recirculation in the basin (Castillo et al., 2015).

In this work, the free falling jet velocity was measured with Large Scale-Particle Image Velocimetry (LS-PIV) technique and with optical fiber equipment. Results were compared with three-dimensional numerical simulations.

In recent years several researchers have analyzed the near-flow field below the impingement point of free falling jets. Table 1 summarizes the main characteristics of experimental and numerical settings. However, the current understanding on this highly-aerated, highly-turbulent flow is still scarce ,and there is lack of experimental study providing detailed benchmark data (Wang et al., 2018).

Although there are progresses of two-phase flows in hydraulic jumps, detailed theoretical and numerical models of the internal flow features have yet to be developed for a wide range of Froude numbers (Bombardelli, 2012).

The submerged hydraulic jump downstream of the impingement point is a particular case with scarce studies. This work needs to be addressed in order to improve this research field. The submerged hydraulic jump generated in the plunge pool has been analyzed with several procedures. The aeration has been measured with optical fiber equipment, obtaining air concentrations, mean velocities, bubble frequencies, and bubbles' mean diameters. Besides this, the mean velocity and turbulent kinetic energy have been measured in the less aerated region of the water

cushion with Acoustic Doppler Velocimeter (ADV). Laboratory data are compared with the numerical simulations carried out using ANSYS CFX (v. 18).

Table 1. Flow conditions and instrumentation in recent studies of the near-flow field below the impingement point of free falling jets.

Authors	**Nozzle diameter (m)**	**Free falling distance (m)**	**Impingement velocity (m/s)**	**Instrumentation**
Chanson et al. (2004)	0.025 0.0125 0.0273	0.1 0.05 0.0273	3.5-4.4 2.42-3.46 1.79-2.49	Prandtl-Pitot tube; hot-film probe; single-tip phase-detection probe
Ma et al. (2010)	0.025	0.10	3.5-4.4	Computational multiphase fluid dynamics (CMFD) code
Qu et al. (2013)	0.06	0.10	2.0-2.5	Particle Image Velocimetry (PIV)
Bertola et al. (2017)	0.012	0.10	2.49-7.43	Dual-tip phase-detection probe; total pressure sensor; Prandtl-Pitot tube; acoustic displacement meter
Boualouache et al. (2017)	0.005	0.01	2.54	ANSYS CFX and Fluent codes
Wang et al. (2018)	0.012	0.05-0.15	2.4-5.5	Dual-tip phase-detection probe; total pressure sensor

2. Material and Methods

2.1. Experimental Device

The Hydraulic Laboratory of the Universidad Politécnica de Cartagena has an experimental device designed for the study of turbulent jets and energy dissipation in overtopping weirs.

The mobile device of the weir has been modified from that used by Carrillo (2014) to improve the energy dissipation in the inlet channel before the weir, to increase the range of flows tested and the discharge heights. The infrastructure is designed to analyze flows between 10 l/s and 200 l/s, discharge heights between 2.20 m and 3.50 m, and different water cushions (Fig. 1b).

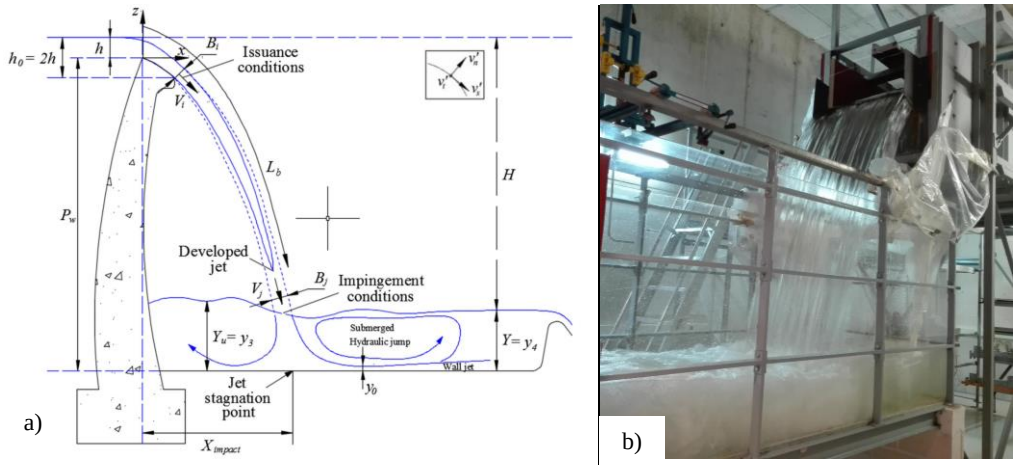

Figure 1. a) Schematic of falling rectangular jets and receiving basin (Castillo et al. 2017); b) Infrastructure of free discharge in laboratory.

The fixed stilling basin is 1.05 m wide, 3.00 m long, and 1.60 m high. It is built in methacrylate to observe the flow inside. It allows different depths of water cushions, from direct impact to depths of 1.00 m.

Pressure measurements are currently being measured with piezoresistive sensors located in the bottom of the plunge pool, together with the study of velocities in different sections of the water cushion using Doppler equipment and aeration rates using optical fiber methodology.

2.2. Optical Fiber

To measure the air concentration in the free-falling jet and in the dissipation basin, an optical fiber equipment with double-tip probe of RBI-Instruments was used. This equipment allows the detection of the phase change between air and water. The rise and fall of the signal detected by the probe are, respectively, the arrival and departure of the gas phase at the sensor tip. The threshold values were set at 1.0 V and 2.5 V (Boes and Hager, 1998). The void fraction is defined as the ratio between the total time the probe is in gas (Σt_{Gi}) and the time duration t of the experiment.

According to Stutz and Reboud (1997a, 1997b), this equipment allows for the measurement of water-air flows with velocities up to 20 m/s. The relative uncertainty of the void fraction is estimated at approximately 15% of the measured value. A source of error in estimating the presence of air in the flow is due to the statistical count of the number of air bubbles in contact with the tips of the probe (Stutz, 1996). Therefore, a short duration of the measurement would contribute to a smaller accuracy of the results.

To evaluate the minimum duration of the measurements, André et al. (2005) analyzed the time required to stabilize the mean value during the measurement and found that the quasi-stationary values were statistically representative of the air concentration. Based on the sensitivity study of the probe behavior, the authors recommend a 60 s sampling sequence as a good compromise between precision and duration of the experiments.

Boes and Hager (2003) carried out experiments with 4000 air bubbles and samplings of 30 s. The authors considered that the accuracy of the air concentration and velocity measurements is related to the variation of the N_b phase, air-water variation or the inverse, rather than the sample duration t.

A sample sequence of 90 s was considered in this study. Fig. 2 shows the evolution of the void fraction until it reaches a relative uncertainty of about 1%, as well as the sum of bubbles detected during the test.

Following these ideas, the two-phase flow characteristics were measured downstream of the stagnation point in different cross-sections spaced 0.10 m.

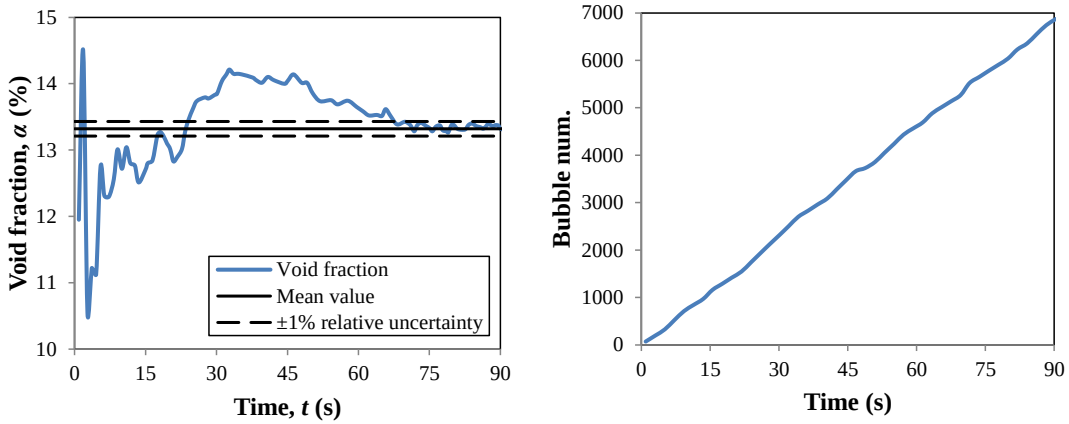

Figure 2. Evolution of the void fraction and the number of bubbles detected by the optical fiber equipment during the test.

2.3. Acoustic Doppler Velocimeter

In this study, the characteristics of the Acoustic Doppler Velocimeter equipment (ADV) were selected considering that the main objective was to characterize the turbulence. We used Nortek A.S. Vectrino Plus equipment. The velocity range was selected as ± 4.00 m/s (the maximum available in the equipment). With this adjustment, the ADV can measure horizontal velocities up to 5.25 m/s and vertical velocity up to 1.50 m/s (maximum jet velocity before impact ≈ 6.75 m/s). Due to the fact that Doppler equipment needs to be fully immersed in water, the first 5-6 cm of the water column could not be measured with this instrumentation.

Turbulent kinetic energy was measured 0.50 m upstream of the weir in inlet of the experimental facility to obtain the boundary conditions in the numerical simulations. This distance ensures that the streamlines are horizontal upstream of the weir in the range of the flows tested (0.50 m > 5*h*).

In the dissipation basin, velocities were recorded in different cross-sections spaced 0.10 m downstream of the stagnation point. In order to characterize the macro-turbulence of the flow, 5000 data were recorded at each measured point using a frequency of 10 Hz (more than 8 minutes of observation).

As the flows are highly turbulent and aerated, the values obtained with ADV may be affected by spurious or "spike" signals. Each time series should be filtered with velocity and acceleration thresholds (Wahl 2000, 2003).

In addition to this, air may also affect the ADV signal. Frizell (2000) analyzed the influence of air concentrations ranging from 0% to 3.61%. As air concentrations and bubble sizes increase, the correlation values decrease drastically as the acoustic signals are absorbed and reflected by the two-phase flow. Matos et al. (2002) also found that air bubbles affect the accuracy of velocity measurements obtained with ADV. However, their experiment results suggest that ADV can provide reasonable estimations of velocity for low air concentrations (up to 8%).

As the flow in the plunge pool is highly turbulent and aerated, the Phase-Space Thresholding filter (Goring and Nikora 2002, modified by Castillo 2009) was used. The spikes were replaced on each record by the mean value of the twelve closest points. Details of the filtering method used may be obtained in Castillo el at. (2017).

2.4. Large Scale-Particle Image Velocimetry

Large-Scale Particle Image Velocimetry (LS-PIV) is an extension of particle image velocimetry (PIV), which provides velocity fields spanning large flow areas in laboratory or field conditions. Additional data, such as mappings of large-scale flow structures and discharges, are readily obtainable using LS-PIV. While the images and data-processing algorithms are similar to the conventional PIV technique, adjustments are required for illumination, seeding procedures, and pre-processing of the recorded images (Fujita et al., 1998). This technique has been used to estimate the velocity of free falling jets (Bercovitz et al., 2016).

In present work, the flow was recorded with a high-speed camera FASTCAM SA3 Model 120K (Photron Limited), a zoom lens with 50 mm focal length by Nikkor, lens aperture f/5.6, 1024x1024 pixels resolution, 8 bits→255 shades, and a horizontal distance from the camera to the jet recorded of around 3.50 m. Hence, the recording window dimensions were around 0.9 m x 0.9 m. Illumination of experiment was reached with 8 regular 800 w light bulbs with reflecting mounts in front of the flow. The speed camera used was 500 Hz; 0.00105 (m/pixel). Frames were analyzed in consecutive pairs by cross-correlation algorithm in an interrogation area of 64 x 64 pixels with sub-windows of 32 x 32 pixels in a single pass search and overlapping of 50% (Adrian and Westerweel, 2010). No background slide subtraction or noise remove techniques were applied. The PIVlab 1.41 software was used for the cross-correlation. This program is an open-source time-resolved particle image velocimetry tool in MATLAB® (Thielicke and Stamhuis, 2014). In each test, 1360 images were recorded and each test was repeated four times. The velocity values were averaged at each sub-window. Fig. 3 shows the velocity field obtained with a pair of images. Distances in the recorded window were calibrated considering a vertical plane located at the toe of the jet, at 3.30 m of horizontal distance to the camera. These distances were projected over the upper nappe profile to achieve the real displacements of the flow, with ratios from 1/1.15 in the upper zone, to 1/1.00 in the lower part of the recorded window. To do this, it was assumed that the shape of the upper nappe profile agrees with that proposed by Scimemi (1930) at each sub-window. The agreement between the lab measurements and the Scimemi (1930) formula was verified by Carrillo (2014). Fig. 3c shows the sub-window length obtained from the projection of each segment in the vertical plane used to calibrate the distance.

2.5. Numerical Simulations

Computational Fluid Dynamics (CFD) allows to solve problems in fluid mechanics, providing great results with great flexibility and speed. However, for its correct application it is necessary to compare and calibrate with results obtained in physical models and/or prototypes.

This work compares the results simulated with ANSYS CFX (v.18.0) and the data obtained in the laboratory. The fluid domain of the study area is divided into control volumes. In each one, the flow parameters (velocity, pressures, etc.) are calculated in discrete times, considering the equilibrium of the Navier-Stokes equations.

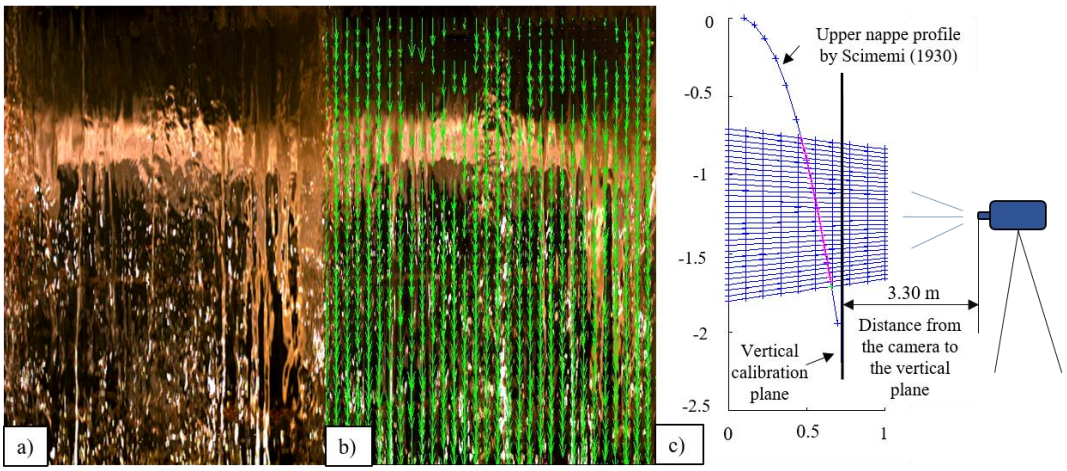

Figure 3. a) Image recorded with 500 Hz frequency; b) Velocity field defined by Cross Correlation PIV technique between a pair of images; c) Scheme of the projection of the vertical segments over the upper nappe profile proposed by Scimemi (1930).

To solve the closure problem, the Shear-Stress-Transport (SST) turbulence model was selected. This model has been designed to obtain greater accuracy in flow separation under adverse pressure gradients (Menter, 1994). The SST model takes into account the precision of the k-ω model in the region close to the walls and changes to the k-ε model in the outer part of the boundary layer. The best behavior of this turbulence model has been demonstrated in numerous validation studies in this type of flows (Carrillo, 2014; Castillo et al., 2014, 2017).

For the resolution of the air-water two-phase flow, the homogeneous model was chosen (ANSYS Inc., 2016). This model can be considered as a limiting case of the inhomogeneous model, where the transfer rate at the interface of both fluids is very large. In this way, it solves the interface considering that in these zones both fluids share the same field of velocities.

A mesh based on hexahedral elements of 0.01 m was used to solve the three-dimensional domain.

The boundary conditions were the water level in the inlet and outlet sections and hydrostatic pressures distributions. In the inlet condition, the turbulence measured in the laboratory with ADV was considered.

A transient calculation of 60 s was considered with a time-step interval of 0.05 s. After 20 s, it is considered that the steady state has been reached, obtaining the average of the different parameters.

The numerical model was previously validated considering the evaluation of the mesh size and the choice of the turbulence model. After the validation process, differences in the mean pressure at the stagnation point and the pressure distribution around it show a maximum error from -4 to 7%. This level of agreement is understandable given the observed air concentrations with the homogeneous-type models (Jha and Bombardelli, 2010; Bombardelli, 2012). Details of the validation and the boundary conditions may be obtained in Carrillo (2014), and Castillo et al., (2014, 2017).

3. Results and Discussion

3.1. Jet velocity

Following a streamline that starts on the weir, Fig. 4a shows the free falling jet velocity when different mesh sizes were considered. The results are compared with optical fiber and LS-PIV measurements. The mesh size has a small influence in the falling jet velocity. Velocity obtained with the different methods tended to be slightly smaller than the free-falling velocity due only to the gravity effects. This indicates the effect of air-water friction. The LS-PIV measurements were less accurate due to the difficulties to illuminate the falling jet. LS-PIV results are in agreement with the measurements carried out by Bercovitz el al. (2016).

3.2. Void Fraction in the Plunge Pool

Fig. 4b shows the void fraction ($\alpha = \Sigma t_{Gi}/t$) obtained by the optical fiber equipment in different cross-sections downstream of the stagnation point (X = horizontal distance to the stagnation point). The largest values of void fraction were obtained close to the impact point of the rectangular jet, reaching values around 15%. As the flow moves away from the impact zone of the jet, the void fraction detected by the probe tends to reduce its value. The profiles located more than X = 0.40 m from the impact point show a void fraction smaller than 8%, reaching values around 3% in the profile located at X = 1.00 m.

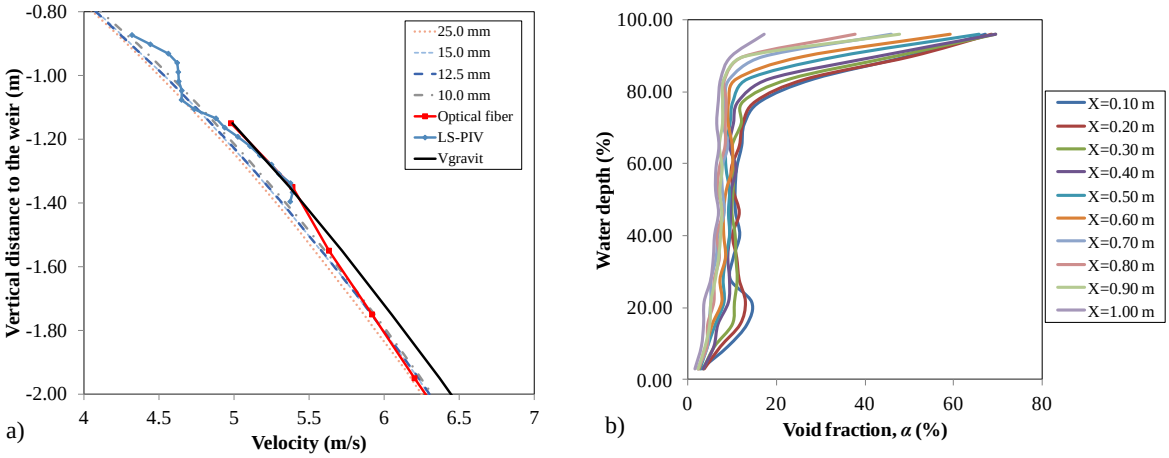

Figure 4. a) Free falling jet velocity (q = 0.058 m^2/s); b) Void fraction downstream of the stagnation point (q = 0.082 m^2/s, H = 2.19, Y = 0.32 m). Distribution of velocities and kinetic energy in the dissipation bowl

The velocity profiles in the forward flow of hydraulic jumps may be compared if they are normalized with a velocity scale equal to the maximum velocity, V_{max}, at any section, and with a length scale δ_l equal to the elevation y from the bottom where the local velocity $V = V_{max}/2$, and the velocity gradient is negative (Rajaratnam, 1965; Wu and Rajaratnam, 1996).

The maximum velocity V_{max} and the length scale δ_1 were obtained in each cross-section of the submerged hydraulic jump. Fig. 5 shows the non-dimensioned velocity profiles in different cross sections located downstream of the stagnation point. Laboratory measurements were obtained with Doppler and optical fiber equipment. Laboratory equipments were used considering their limitations. The Doppler measurements were obtained for X > 0.40 m. Upstream this section, the air concentration was higher than 8% and the Doppler equipment did not allow to obtain valid results (see Matos et al., 2002). On the other hand, beyond section X = 0.40 m and above y/δ_1 > 1.5-2.0, the flow was non-unidirectional and the optical fiber obtained erratic values.

In the same cross sections, the results of the CFD simulations were obtained. In general, the results of the numerical simulations show the same behavior as the values obtained in the laboratory.

Fig. 5 also shows the turbulent kinetic energy (TKE) obtained in different sections of the plunge pool with the ADV equipment. The turbulent kinetic energy tends to dissipate quickly as the as the flow moves away from the impact zone, reaching maximum values around 0.30 m^2/s^2 in the profile located 0.80 m from the stagnation point. The results obtained with the turbulence model follow the evolution of energy dissipation (Castillo et al., 2017).

3.3. Bubbles Frequency and Size in the Plunge Pool

The frequency of the bubbles detected by the probe has been analyzed by different authors in hydraulic jumps (Murzyn et al., 2005; Murzyn and Chanson, 2007).

Fig. 6 shows the frequency of bubbles detected by the probe. In most of the profiles, the highest values are obtained in the vicinity of the bottom. In the profile located 0.10 m downstream of the stagnation point, a maximum of 8700 bubbles were detected with a frequency of 96 Hz. The maximum values tend to reduce as the flow moves from the impact zone of the jet. In the profile X = 1.00 m, the values tend to be constant in all the depth, with a detection frequency of bubbles around 30 Hz.

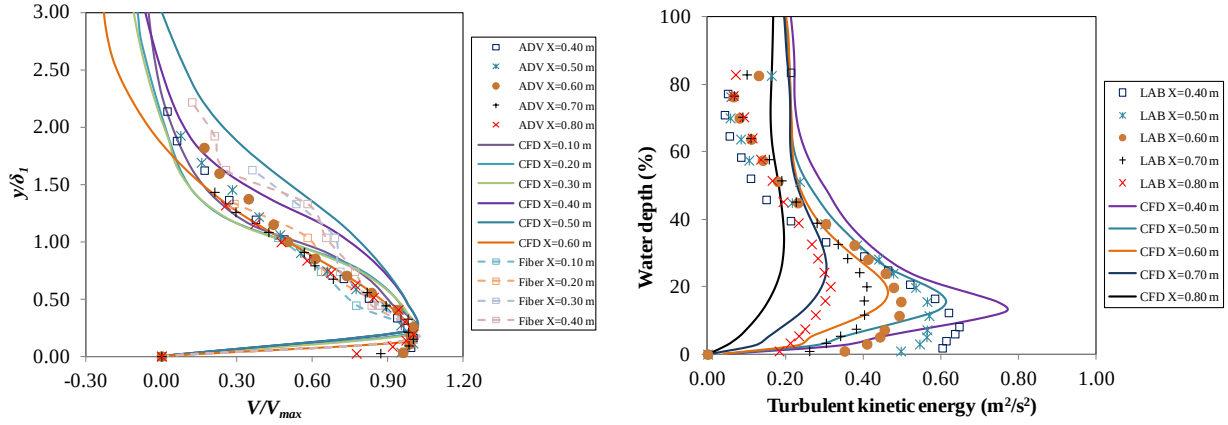

Figure 5. Profiles of horizontal mean velocity and turbulent kinetic energy in different sections of the plunge pool (q = 0.082 m^2/s, H = 2.19, Y = 0.32 m).

These values are similar to the results measured by Murzyn et al. (2005), who obtained maximum frequencies around 85 Hz in hydraulic jumps with a Froude number of 4.82, and by Murzyn and Chanson (2007), who recorded maximum frequencies around 120 Hz for hydraulic jumps with Froude number of 8.30.

Assuming the hypothesis that bubbles are spherical, equally distributed in the time and that their movement is unidirectional, the size of the bubbles detected by the optical fiber equipment may be characterized by the mean diameter of Sauter, d_s (Clift et al. 1978, RBI-Instrumentation 2012). This is the diameter of the bubbles whose volume/surface ratio is the same that the calculated for all the bubbles detected during the test. The mean diameter of Sauter may be calculated as:

$$d_s = \frac{3\alpha u}{2F} \tag{1}$$

where α is the void fraction, u the mean velocity of the bubbles, and F the bubble detection frequency.

Considering the velocity profiles in the previous section, Fig. 6 also shows the size of the bubbles detected in different sections of the plunge pool. Beyond section X = 0.40 m the flow is non-unidirectional and Ec. (1) may not be used. Mostly values are below 6 mm, with maximum values around 10 mm. These diameters are slightly lower than the results obtained by Murzyn et al. (2005) and by Murzyn (2010) in hydraulic jumps.

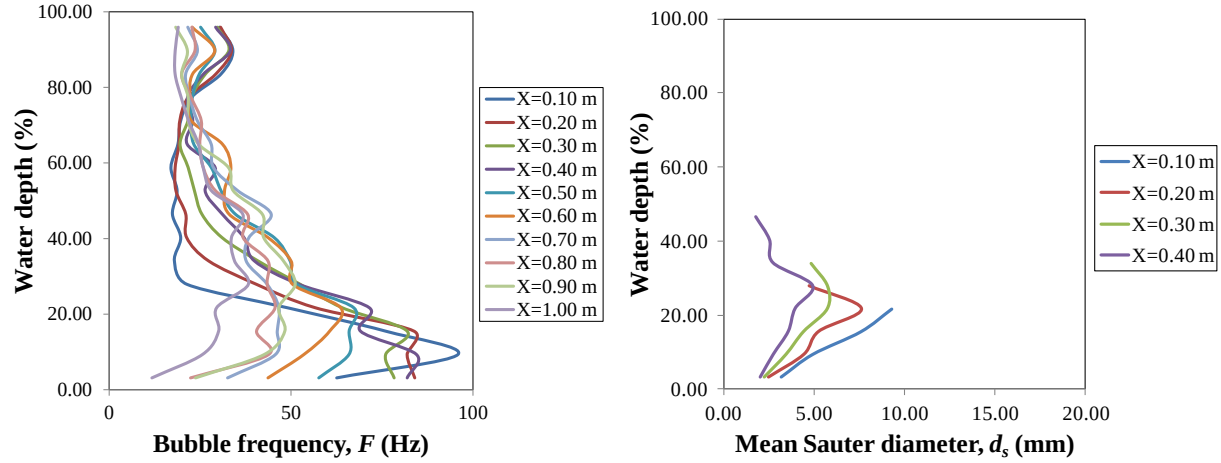

Figure 6. Frequency and mean diameter of bubbles detected downstream of the stagnation point (q = 0.082 m^2/s, H = 2.19, Y = 0.32 m).

4. Conclusions

To observe and to predict two-phase flows in hydraulic structures is very complicated because of the undiluted nature of the flow. Under these conditions, the experimental data, and the results of the simulations are difficult to compare in a clear way.

In this work we have analyzed the characteristics of the air-water flow produced downstream of a free spillway. Using uniform illumination, the LS-PIV methodology may be used to estimate the velocity of the free falling jet.

Optical fiber and ADV equipment were used considering their limitations. In this way, the velocity profiles of the complete hydraulic jump could be measured. The optical fiber measurements complement the flow velocity obtained in previous studies (Castillo et al., 2017).

There are scarce data of air entrainment in submerged hydraulic jumps downstream of free falling jets. In general, the characteristics of the air-water flow (void fraction, bubble frequency, and size) are similar to those observed by different researchers in hydraulic jumps.

The CFD simulations provided results close to the values measured in the laboratory, despite having used a simple two-phase flow model. The "homogeneous" model seems to be able to predict the phenomenon.

In order to advance in the knowledge, we plan to study the behavior of two-phase flows in the plunge pool with different experimental techniques. In addition, the laboratory results will be compared with several CFD codes (open source and commercial codes).

5. Acknowledgments

The authors would like to thank the Ministerio de Ciencia e Innovación of Spain and Fondos Europeos de Desarrollo Regional (FEDER), through Project BIA2011-28756-C03-02. They acknowledge the helpful comments of the anonymous reviewers.

6. References

Adrian, R.J., and Westerweel, J. (2010). Particle Image Velocimetry. Cambridge University Press: Cambridge, UK.

André, S., Boillat, J.L., and Schleiss, A.J. (2005). "Discussion of 'Two-phase flow characteristics of stepped spillways' by Robert M. Boes and Willi H. Hager." *Journal of Hydraulic Engineering,* 131(5), 423–427.

Annandale, G.W. (2006). Scour Technology. Mechanics and Engineering Practice. McGraw-Hill, New York.

ANSYS Inc. (2016). ANSYS CFX. Reference Guide. Release 18.0.

Bercovitz, Y., Lebert, F., Jodeau, M., Buvat, C., Violeau, D., Pelaprat, L. and Hajczak, A. (2016). "LS-PIV procedure applied to a plunging water jet issuing from an overflow nappe." *Proceedings of the 4th IAHR Europe Congress. Sustainable Hydraulics in the Era of Global Change,* Liege, Belgium, 166–173.

Bertola, N., Wang, H., and Chanson, H. (2017). "A physical study of air–water flow in planar plunging water jet with large inflow distance". *International Journal of Multiphase Flow.* (in press).

Boes, R., and Hager, W.H. (1998). "Fiber-optical experimentation in two-phase cascade flow." *Proceedings of the International RCC Dams Seminar (K. Hansen, ed.)*. Denver, CD, USA.

Boes, R., and Hager, W.H. (2003). "Two-phase flow characteristics of stepped spillways." *Journal of Hydraulic Engineering*, 129(9), 661–670.

Bombardelli, F.A. (2012). "Computational multi-phase fluid dynamics to address flows past hydraulic structures." *Proceedings of the* 4th IAHR International Symposium on Hydraulic Structures, 9-11 February 2012, Porto, Portugal, ISBN: 978-989-8509-01-7.

Boualouache, A., Zidouni Kendil, F., and Mataoui, A. (2017). "Numerical assessment of two phase flow modeling using plunging jet configurations". *Chemical Engineering Research and Design*, 128, 248-256.

Carrillo, J.M. (2014). Metodología numérica y experimental para el diseño de los cuencos de disipación en el sobrevertido de presas de fábrica. PhD Thesis. Universidad Politécnica de Cartagena, Spain (in Spanish).

Castillo, L.G. (2009). "Measurement of velocities and characterization of some parameters inside of free and submerged hydraulic jumps." *Proceedings of 33rd International Association of Hydraulic Engineering & Research Congress*, Vancouver, Canada.

Castillo, L.G., and Carrillo, J.M. (2017). "Comparison of methods to estimate the scour downstream of a ski jump." *International Journal of Multiphase Flow*, 92, 171-180.

Castillo, L.G., Carrillo, J.M., and Blázquez, A. (2015). "Plunge pool mean dynamic pressures: a temporal analysis in nappe flow case." *Journal of Hydraulic Research,* 53(1), 101–118.

Castillo, L.G., Carrillo, J.M., and Bombardelli, F.A. (2017). "Distribution of mean flow and turbulence statistics in plunge pools." *Journal of Hydroinformatics*, 19(2), 173-190.

Castillo, L.G., Carrillo, J.M., and Sordo-Ward, A. (2014). "Simulation of overflow nappe impingement jets." *Journal of Hydroinformatics*, 16(4), 922–940.

Chanson, H., and Brattberg, T. (2000). "Experimental study of the air-water shear flow in a hydraulic jump." *International Journal of Multiphase Flow*, 26, 583-607.

Chanson, H., Aoki, S., and Hoque, A. (2004). "Physical modelling and similitude of air bubble entrainment at vertical circular plunging jets." *Chemical Engineering Science*, 59, 747 – 758.

Clift, R., Grace, J.R., and Weber, M.E. (1978). Bubbles, drops and particles. Academic Press, New York.

FEMA. (2014). Technical Manual: Overtopping Protection for Dams. Federal Emergency Management Agency. FEMA P-1014, May. US Department of Homeland Security, USA.

Frizell, K.W. (2000). "Effects of aeration on the performance of an ADV." *2000 Joint Conf. on Water Resources Engineering and Water Resources Planning & Management* (R. H. Hotchkiss & M. Glade, eds). ASCE, Minneapolis, USA, (CD-ROM).

Fujita, I., Muste, M., and Kruger, A. (1998). "Large-scale particle image velocimetry for flow analysis in hydraulic engineering applications." *Journal of Hydraulic Research*, 36(3), 397-414.

Goring, G., and Nikora, V. (2002). "Despiking acoustic Doppler velocimeter data." *Journal of Hydraulic Engineering*, 128 (1), 117–126.

Jha, S. K., and Bombardelli, F.A. (2010). "Toward two-phase flow modeling of non-dilute sediment transport in open channels." *J. Geophys. Res. Earth Surf.* 115 (F3), 2003–2012.

Ma, J., Oberai, A.A., Drew, D.A., Lahey Jr., R.T., and Moraga, F.J. (2010). "A quantitative sub-grid air entrainment model for bubbly flows – plunging jets." *Computers & Fluids*, 39, 77–86.

Matos, J., Frizell, K.H., Andre, S., and Frizell, K.W. (2002). "On the performance of velocity measurement techniques in air-water flows." *Hydraulic Measurements and Experimental Methods Conference 2002* (T. L. Wahl, C. A. Pugh, V. A. Oberg & T. B. Vermeyen, eds). ASCE, Estes Park, CO, USA.

Menter, F.R. (1994). "Two-equation eddy-viscosity turbulence models for engineering applications." *The American Institute of Aeronautics and Astronautics Journal,* 32(8), 1598–1605.

Murzyn, F. (2010). "Assessment of different experimental techniques to investigate the hydraulic jump: do they lead to the same results?" *3rd International Junior Researcher and Engineer Workshop on Hydraulic Structures*, May 02-04, Edinburg, UK, 3-36.

Murzyn, F., and Chanson, H. (2007). Free Surface, Bubbly flow and Turbulence Measurements in Hydraulic Jumps. Report CH63/07, Division of Civil Engineering, The University of Queensland, Brisbane.

Murzyn, F., Mouaze, D., and Chaplin, J.R. (2005). "Optical fibre probe measurements of bubble flow in hydraulic jumps." *International Journal of Multiphase Flow*, 31, 141-154.

Qu, X., Goharzadeh, A., Khezzar, L., and Molki, A. (2013). "Experimental characterization of air-entrainment in a plunging jet". *Experimental Thermal and Fluid Science*, 44, 51-61.

Rajaratnam, N. (1965)." The hydraulic jump as wall jet." *Proc. ASCE J. Hydraul. Div. 91 (HY5)*, 107–132.

RBI-Instrumentation. (2012). ISO Software user's guide.

Scimemi, E. (1930). "Sulla Forma delle Vene Tracimanti." *L'Energia Elettrica*, 7(4), 293-305. (in Italian).

Stutz, B., and Reboud, J.L. (1997a). "Experiment on unsteady cavitation." *Experiments in Fluids,* 22, 191–198.

Stutz, B., and Reboud, J.L. (1997b). "Two-phase flow structure of sheet cavitation." *Physics of Fluids*, 9(12), 3678–3686.

Stutz, B. (1996). Analyse de la structure diphasique et instationnaire de poches de cavitation (Analysis of the two Phases and Non-Permanent Structure of Cavitation Bubbles). PhD Thesis, Institut National Polytechnique de Grenoble, France (in French).

Thielicke, W., and Stamhuis, E. (2014). “PIVlab–towards user-friendly, affordable and accurate digital particle image velocimetry in MATLAB.” *Journal of Open Research Software*, 2(1).

Wahl, T.L. (2000). "Analyzing ADV data using WinADV." *Joint Conference on Water Resources Engineering and Water Resources Planning & Management*, July 30–August 2, Minneapolis, MN.

Wahl, T.L. (2003). "Discussion of ‘Despiking acoustic Doppler velocimeter data’ by Derek G. Goring and Vladimir I. Nikora." *Journal of Hydraulic Engineering*, 129 (6), 484–487.

Wahl, T.L., Frizell, K.H., and Cohen, E.A. (2008). "Computing the trajectory of free jets." *Journal of Hydraulic Engineering*, 134(2), 256–260.

Wang, H., Slamet, N.S., Zhang, G., and Chanson, H. (2018)." Intrusive measurements of air-water flow properties in highly turbulent supported plunging jets and effects of inflow jet conditions." *Chemical Engineering Science*, 177, 245–260.

Wu, S., and Rajaratnam, N. (1996). "Transition from hydraulic jump to open channel flow." *Journal of Hydraulic Engineering*, 122(9), 526–528.